

Oxidation of Nickel and Ni-Cr and Ni-Na Alloys at High Temperatures

S. Mrowec¹ and Z. Grzesik^{1*}, B. Rajchel²

¹*Department of Solid State Chemistry, Faculty of Materials Science and Ceramics, University of Science and Technology, al. A. Mickiewicza 30, 30-059 Krakow, Poland*

²*Institute of Nuclear Physics, Polish Academy of Science, ul. Radzikowskiego 152, 31-342 Krakow, Poland*

(Received January 26, 2004)

ABSTRACT

Oxidation kinetics of high purity nickel, as well as the nonstoichiometry and chemical diffusion in nickel oxide, have been studied as a function of temperature (1373-1673 K) and oxygen pressure (10^{-10} Pa) using modern microthermogravimetric techniques. In order to eliminate the possible participation of grain boundary diffusion in scale growth at lower temperatures, the oxidation rate measurements have always been started at highest temperature (1673 K) when coarse-grained scale was formed and the temperature and pressure dependence of the oxidation rate was determined by step-wise lowering the temperature of such pre-oxidized sample. Nonstoichiometry and chemical diffusion coefficient in Ni_{1-y}O have also been determined on coarse-grained oxide samples, obtained by complete oxidation of nickel at highest temperature (1673 K). It has been found that under such conditions the parabolic rate constant of nickel oxidation is the following function of temperature and oxygen pressure:

$$k_p = 0.142 \cdot p_{\text{O}_2}^{1/6} \cdot \exp\left(-\frac{239 \text{ kJ/mol}}{RT}\right).$$

The results of nonstoichiometry and chemical diffusion measurements, in turn, may be described by the following relationships:

$$y = 0.153 \cdot p_{\text{O}_2}^{1/6} \cdot \exp\left(-\frac{80 \text{ kJ/mol}}{RT}\right) \quad \text{and} \quad \bar{D} = 0.186 \cdot \exp\left(-\frac{152 \text{ kJ/mol}}{RT}\right).$$

The parabolic rate constants of nickel oxidation, calculated from nonstoichiometry and chemical diffusion data, are in excellent agreement with experimentally determined k_p values, clearly indicating that the predominant defects in nonstoichiometric nickel oxide are double ionized cation vacancies and electron holes and the oxide scale on nickel grows by the outward volume diffusion of cations. It has been shown that the oxidation of Ni-Cr and Ni-Na alloys, like that of pure nickel, follows also parabolic rate law being thus diffusion controlled. In agreement with the defect model of Ni_{1-y}O it has been found that the oxidation rate of Ni-Cr alloy is higher than that of pure nickel, the reaction rate is pressure independent and the activation energy of this process is lower. This implies that the concentration of doubly ionized cation vacancies in $\text{Ni}_{1-y}\text{O}-\text{Cr}_2\text{O}_3$ solid solution is fixed on the constant level by trivalent chromium ions, substitutionally incorporated into cation sublattice of this oxide. In the case of Ni-Na alloy, on the other hand, the oxidation rate is lower than that of pure nickel, the activation energy is higher and the oxidation rate increases more rapidly with oxygen pressure. These

* Corresponding author.

e-mail: grzesik@uci.agh.edu.pl

Fax number: +48 12-6172493

results can again be explained in terms of doping effect, by assuming that univalent sodium ions dissolve substitutionally in cation sublattice of nickel oxide.

Keywords: thermogravimetry; nickel oxide; doping effect; defects; diffusion

1. INTRODUCTION

Defect structure and transport properties of nickel oxide, as well as the kinetics and mechanism of nickel oxidation have been extensively studied by different authors using various experimental techniques /1-15/. This great interest in physicochemical properties of nickel - oxygen system results mainly from both, the important influence of nickel on the oxidation resistance of high temperature alloys, and the model character of nickel oxide in studies of semiconducting properties of transition metal oxides. It has been found that nickel oxide, showing rock-salt structure, is a metal deficit p-type semiconductor (Ni_{1-y}O), the predominant defects being cation vacancies and electron holes. However, the nonstoichiometry, y , in this oxide is very low, not exceeding – even at very high temperatures – 10^{-1} at % ($y < 0.001$). Thus, the determination of nonstoichiometry as a function of temperature and oxygen pressure is very difficult and consequently the results obtained by various authors differ considerably. Some authors claim, namely, that cation vacancies in the discussed oxide are doubly ionized and others insist that even at high temperatures the defect structure is more complex, the predominant defects being singly and doubly ionized cation vacancies in comparable concentrations /15/. Also, the results of oxidation kinetics, obtained by different authors, are inconsistent, making impossible the formulation of univocal conclusions concerning the oxidation mechanism of pure nickel and binary nickel-base alloys at high temperatures. Our experience in this area of research leads to the conclusion that this disagreement in the literature results mainly from the influence of impurities on the kinetics of nickel oxidation, as well as on pressure and temperature dependence of nonstoichiometry in Ni_{1-y}O . This conclusion is in agreement with very careful and detailed analysis of the problem in

question carried out by Rapp /16/ and Kofstad /3/.

The aim of the present paper is an attempt to solve this important problem in studying the oxidation kinetics of very high purity nickel, as well as of binary nickel base Ni-Cr and Ni-Na alloys, as a function of temperature and oxygen activity.

2. MATERIALS AND EXPERIMENTAL PROCEDURE

High purity nickel (99.999 at %) has been used as a starting material for both the oxidation rate measurements of nickel metal, and for obtaining Ni_{1-y}O samples to determine deviations from stoichiometry and chemical diffusion in this oxide. The specimens in the form of rectangular plates (10×15 mm) with a thickness from 0.1 up to 1 mm were polished with emery papers and diamond pastes to obtain mirror like surfaces. The oxidation of nickel and the re-equilibration kinetics of nickel oxide have been studied thermogravimetrically as a function of temperature (1373-1673 K) and oxygen pressure (10^{-5} Pa) in the apparatus shown schematically in Fig. 1. The weight gains of oxidized metal samples or mass changes of re-equilibrated oxide ones have been followed continuously as a function of time with the accuracy of the order of 10^{-7} g. The partial pressure of oxygen in the He-Ar- O_2 gas mixture, flowing through the reaction chamber, was obtained by suitable composition of this atmosphere of the total pressure of 10^5 Pa.

The application of two carrier gases (helium and argon) needs some explanation. If only one carrier gas is used to obtain oxidizing gas mixture, the Archimedes effect is to be expected when the oxygen partial pressure in such mixture is changed. If, namely, the oxygen pressure in Ar- O_2 gas mixture is decreased, the weight of the sample apparently decreases, because of the higher density of argon as compared to oxygen. As a consequence, the registered weight gains of oxidized samples are lower than those resulting from the oxidation process. On the other hand, in He- O_2 atmosphere the opposite effect should be observed. This problem has not been taken into account in previous works published in literature and can be considered as a second source of inadequate results in addition to the

influence of impurities. In order to eliminate this systematic error, the Ar/He ratio was chosen in such a way, that the density of this carrier gas mixture was exactly the same as that of oxygen. The elimination of the discussed error is important in both the determination of the pressure dependence on the metal oxidation kinetics and in evaluation of nonstoichiometry of the oxide as a function of oxygen activity.

The experimental procedure in studying the nickel oxidation kinetics, as well as the re-equilibration rate measurements of Ni_{1-y}O , was as follows. The metal sample was suspended on the microbalance in the reaction chamber and the flow of gas mixture of the suitable composition was started. Simultaneously, the reaction furnace, moved down below the reaction zone, was heated to the temperature at which the sample was to be oxidized. When the desired partial pressure of oxygen in the reaction chamber was established, the furnace was raised to reaction position (see Fig. 1) and weight gains of the sample were continuously registered as a function of time. This procedure was repeated several times at different temperatures and partial pressures of oxygen in order to determine the dependence of the oxidation rate on these two parameters. In addition to kinetic measurements, marker experiments have been carried out in order to prove that coarse-grained Ni_{1-y}O scale layer on nickel is growing

only as a result of outward diffusion of cations.

The nonstoichiometry of Ni_{1-y}O has been determined as a function of temperature and oxygen pressure in the following way. Nickel sample suspended in the microthermogravimetric apparatus was completely oxidized at highest temperature (1673 K) and oxygen pressure (10^5 Pa) and when constant weight of the oxide sample was reached, the nonstoichiometry, y , was calculated through the following empirical formula:

$$y = 1 - \frac{m_{\text{Ni}} \cdot M_{\text{O}}}{m_{\text{O}} \cdot M_{\text{Ni}}} \quad (1)$$

where m_{Ni} and m_{O} denote masses of the nickel sample and consumed oxygen, respectively; and M_{Ni} and M_{O} atomic masses of nickel and oxygen, respectively. Subsequently, the partial pressure of oxygen was changed step by step to lower values and after reaching in every step the thermodynamic equilibrium, the nonstoichiometry of Ni_{1-y}O was calculated. This procedure was repeated several times at lower and lower temperatures.

During these experiments the chemical diffusion coefficient in Ni_{1-y}O has also been determined from re-equilibration kinetics of oxide samples when going from one thermodynamic equilibrium state to another. When, namely, the oxygen pressure at the given temperature was suddenly changed to the lower value, the sample gradually lost weight as a result of the evolution of oxygen to the environment and the liberated electrons and cations filled electron holes and cations vacancies, respectively. As a consequence, between the surface and the interior of the sample, the concentration gradient of ionic and electronic defects was established, resulting in their ambipolar outward diffusion. When on the other hand, the oxygen pressure was suddenly changed to a higher value, oxygen atoms are bonded on the sample surface with the electrons and cations diffusing there from the interior of the lattice and leaving behind electron holes and cation vacancies, respectively. Thus, the weight of the sample, and thereby point defect concentration in the oxide, increases. From such oxidation and reduction runs chemical diffusion coefficient, \bar{D} , could have been calculated as a function of temperature and oxygen pressure, using the following

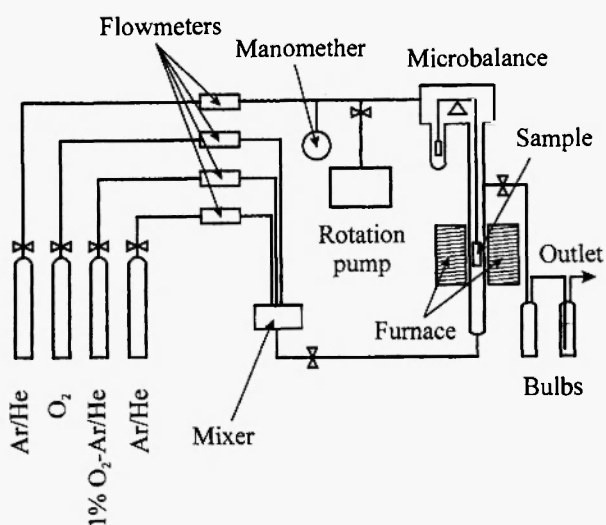


Fig. 1: Microthermogravimetric apparatus for studying the kinetics of solid-oxygen interactions at high temperatures.

solution of the second Fick's law /17, 18/:

$$1 - \frac{\Delta m_t}{\Delta m_k} = \frac{8}{\pi^2} \exp\left(-\frac{\bar{D}\pi^2 t}{4l^2}\right) \quad (2)$$

where Δm_t denotes the weight change of the oxide sample after time t , and Δm_k is the total weight change when new equilibrium state is established, and l denotes one half of the sample thickness. It should be noted that correct values of chemical diffusion coefficient could only be obtained if no hysteresis between oxidation and reduction runs was obtained, i.e. when the slowest step of the overall re-equilibration kinetics was the ambipolar diffusion of cation vacancies and electron holes. This, in fact, has been proved in our experiments. The details of re-equilibration kinetic method used in this work were described elsewhere /19, 20/.

High purity nickel (99.999 at %) and chromium (99.999 at %) were used as starting materials to obtain Ni-Cr alloy, containing 1 % at of chromium. Nickel and chromium powders were mixed in agate mortar and melted in arc-furnace under high purity argon atmosphere. The melting procedure was repeated several times in order to obtain homogeneous alloy. In agreement with Ni-Cr phase diagram, it has been found that this alloy was singly-phase solid solution. The ingots were cut into slices using the diamond saw. The specimens in the form of flat discs, with the diameter of 1.5 cm and the thickness from 0.03 up to 0.1 cm, were polished with emery papers and diamond pastes to obtain mirror-like surfaces.

Ni-Na alloys of acceptable quality are very difficult to be prepared by conventional metallurgical procedure. Thus, some amount of sodium was implanted into the surface layer of nickel specimen, using acceleration energy of Na^+ ions of 25 keV. The dose applied was $10^{17} \text{ Na}^+ \text{ ions/cm}^2$.

The oxidation kinetics of these alloys have been studied thermogravimetrically as a function of temperature (1373 - 1673 K) and oxygen pressure (10^{-10} - 10^5 Pa) using the same experimental procedure as in the case of pure nickel oxidation.

3. RESULTS AND DISCUSSION

In agreement with the literature data it has been found that the oxide scale on nickel is growing by the outward diffusion of cations (marker at the metal-scale interface). In order to eliminate the possible participation of grain boundary diffusion in scale growth at lower temperatures, oxidation rate measurements have always been started at highest temperature (1673 K) when coarse grained scale was formed. Further kinetic runs have been determined by step-wise lowering the temperature of such pre-oxidized samples in order to obtain the results at lower temperatures on coarse grained oxidation product, in which the participation of grain-boundary diffusion is unimportant. In fact, this problem, in addition to impurity and Archimedes effects, has not been taken into account in previous works.

It has been found that in the whole temperature and pressure range the oxidation process follows strictly the familiar parabolic rate law being thus diffusion controlled. This is illustrated in Fig. 2, showing parabolic plots at 1673 K for several oxygen pressures. Analogous results have been obtained at other temperatures and oxygen pressures. Figs. 3 and 4, in turn, show the temperature and pressure dependence of

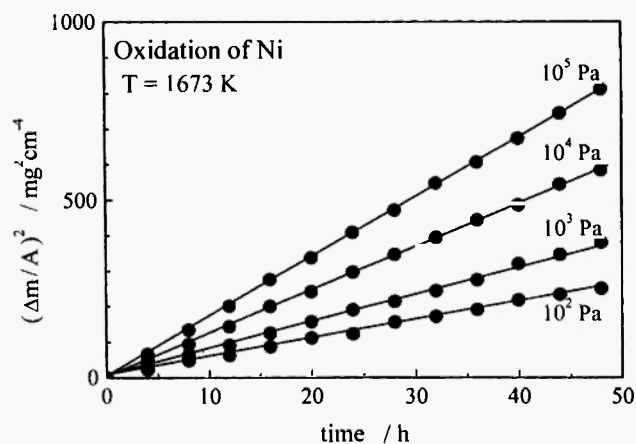


Fig. 2: The oxidation kinetics of nickel at 1673 K for several oxygen pressures.

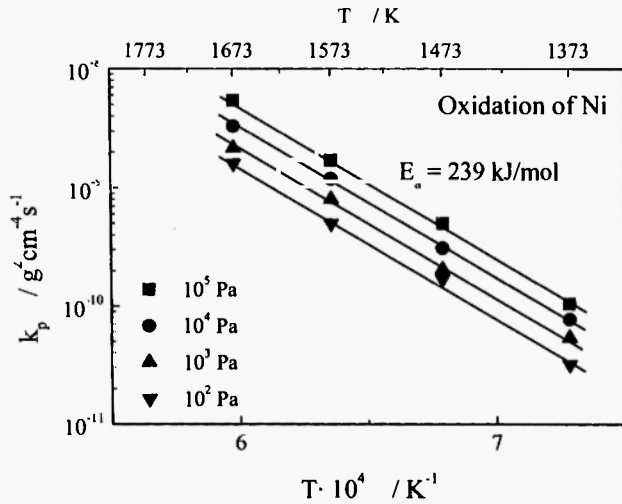


Fig. 3: The temperature dependence of the parabolic rate constant of nickel oxidation for several oxygen pressures.

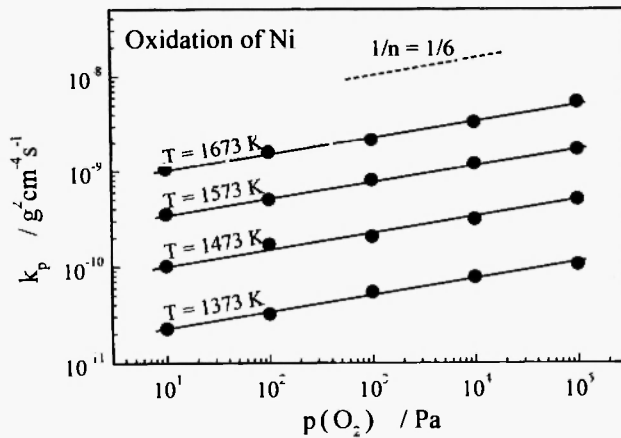


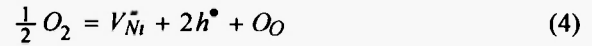
Fig. 4: The pressure dependence of the parabolic rate constant of nickel oxidation for several temperatures.

the parabolic rate constant of nickel oxidation, presented in Arrhenius and double-logarithmic plots, respectively. It follows from these diagrams that the activation energy of oxidation does not change with oxygen pressure and the pressure dependence of the oxidation rate is temperature independent. Thus, the parabolic rate constant of nickel oxidation, as dependent on temperature and oxygen pressure, may be described by the following empirical equation:

$$k_p = 0.142 \cdot p_{O_2}^{1/6} \cdot \exp\left(-\frac{239 \text{ kJ/mol}}{RT}\right) \quad (3)$$

where k_p is the parabolic rate constant of nickel oxidation expressed in $\text{g}^2 \text{cm}^{-4} \text{s}^{-1}$.

From Wagner's theory of metal oxidation it follows that, if the mobility of predominant point defects in the growing scale is independent on their concentration, the parabolic rate constant of metal oxidation is the same function of oxygen pressure as that of nonstoichiometry of the oxide forming the scale [21, 22]. Thus, the pressure dependence of k_p described by eq. (3) suggests that the predominant defects in Ni_{1-y}O are double ionized cation vacancies and electron holes. This simple defect situation is described by the following quasi-chemical reaction:



(The Kröger-Vink notation of defects is used throughout this paper [23]). Applying to this defect equilibrium the mass action law:

$$K_{V^{\bullet\bullet}} = [V_{\text{Ni}}^{\bullet\bullet}] \cdot [h^{\bullet}]^2 \cdot p_{O_2}^{-1/2} \quad (5)$$

and the appropriate electroneutrality condition:

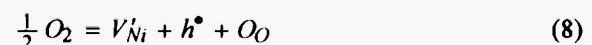
$$2[V_{\text{Ni}}^{\bullet\bullet}] = [h^{\bullet}] \quad (6)$$

one obtains the following relationship, describing the dependence of nonstoichiometry and thereby defect concentration on oxygen pressure and temperature:

$$\begin{aligned} y = [V_{\text{Ni}}^{\bullet\bullet}] &= \frac{1}{2} [h^{\bullet}] = \left(\frac{1}{4} K_{V^{\bullet\bullet}}\right)^{1/3} p_{O_2}^{1/6} \\ &= 0.63 p_{O_2}^{1/6} \exp\left(\frac{\frac{1}{3} \Delta S_f}{R}\right) \exp\left(-\frac{\frac{1}{3} \Delta H_f}{RT}\right) \end{aligned} \quad (7)$$

where ΔS_f and ΔH_f are entropy and enthalpy of defect formation, respectively.

If singly ionized cation vacancies would predominate, the following defect equilibrium should be considered:



and applying again the mass action law:

$$K_{V'} = [V_{Ni}'] \cdot [h^\bullet] \cdot p_{O_2}^{-1/2} \quad (9)$$

and the appropriate electroneutrality condition:

$$[V_{Ni}'] = [h^\bullet] \quad (10)$$

such a dependence of nonstoichiometry and thereby defect concentration on oxygen pressure and temperature should be expected:

$$\begin{aligned} y = [V_{Ni}'] &= [h^\bullet] = K_{V'}^{1/2} \cdot p_{O_2}^{1/2} \\ &= p_{O_2}^{1/4} \exp\left(\frac{\frac{1}{2}\Delta S_f}{R}\right) \exp\left(-\frac{\frac{1}{2}\Delta H_f}{RT}\right) \end{aligned} \quad (11)$$

Finally, if doubly and singly ionized vacancies were to predominate in comparable amounts, as suggested by several authors in the literature [24], the combination of eqs. (4) and (8) and the application of appropriate electroneutrality condition:

$$[V_{Ni}'] + [V_{Ni}^{*}] = \frac{2}{3} [h^\bullet] \quad (12)$$

leads to the following dependence of nonstoichiometry on oxygen pressure:

$$y = [V_{Ni, total}] = \text{const} \cdot p_{O_2}^{1/6} \exp\left(-\frac{E}{RT}\right) \quad (13)$$

In order to verify the conclusion concerning the degree of defect ionization resulting from the pressure dependence of k_p (eq. (3)), the nonstoichiometry and the mobility of point defects in $Ni_{1-y}O$ should have been examined. In agreement with theoretical predictions, it has been found that the nonstoichiometry, and thereby defect concentration in $Ni_{1-y}O$ is, in the whole temperature range studied, the same function of oxygen pressure as that of parabolic rate constant of nickel oxidation (Figs. 5 and 6) and may be described by the following empirical equation:

$$y = [V_{Ni}'] = 0.153 \cdot p_{O_2}^{1/6} \cdot \exp\left(-\frac{80 \text{ kJ/mol}}{RT}\right) \quad (14)$$

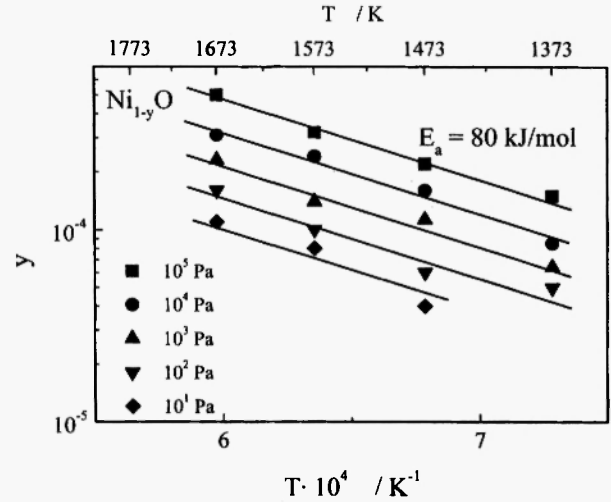


Fig. 5: The temperature dependence of deviation from stoichiometry, y , in $Ni_{1-y}O$ for several oxygen pressures.

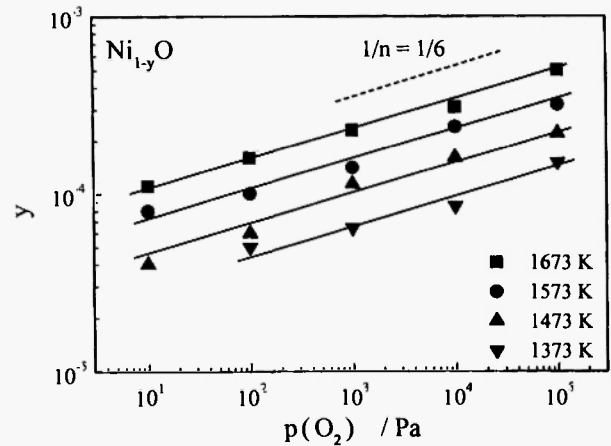


Fig. 6: The pressure dependence of non-stoichiometry, y , in $Ni_{1-y}O$ for different temperatures.

From the comparison of this empirical relationship with theoretical eq.(7), the enthalpy and entropy of the formation of double ionized cation vacancies in $Ni_{1-y}O$ could be calculated: $\Delta H_f = 240 \text{ kJ/mol}$, $\Delta S_f = -35.3 \text{ J/mol}\cdot\text{K}$.

In addition, re-equilibration rate measurements have demonstrated that the chemical diffusion coefficient calculated through eq. (2) and thereby defect mobility in $Ni_{1-y}O$ does not depend on their concentration (Figs. 7 and 8) and its temperature dependence may be described

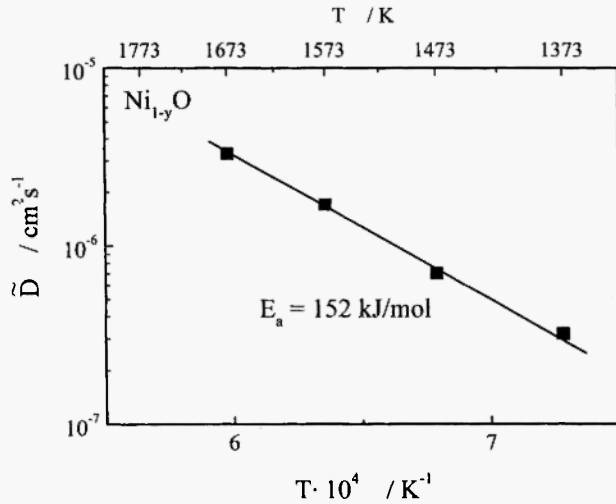


Fig. 7: Dependence of chemical diffusion coefficient, \tilde{D} , in Ni_{1-y}O on temperature.

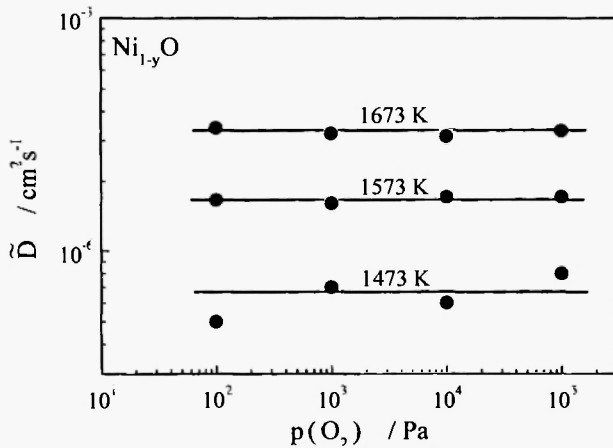


Fig. 8: Dependence of chemical diffusion coefficient, \tilde{D} , in Ni_{1-y}O on oxygen pressure.

by the following empirical equation:

$$\begin{aligned} \tilde{D} &= \text{const} \cdot \exp\left(-\frac{\Delta H_m}{RT}\right) \\ &= 0.186 \cdot \exp\left(-\frac{152 \text{ kJ/mol}}{RT}\right) \end{aligned} \quad (15)$$

From eq. (15) it follows that the activation enthalpy of defect diffusion, $\Delta H_m = 152 \text{ kJ/mol}$.

All these experiments showed clearly that in the whole temperature and pressure range studied, the

predominant defects in nickel oxide are non-interacting, doubly ionized cation vacancies and electron holes, in agreement with the conclusion resulting from the oxidation rate measurements of nickel (eq. (3)). In order to obtain subsequent proof of this conclusion, Wagner's theory of metal oxidation has been applied to calculate the parabolic rate constant of nickel oxidation from nonstoichiometry and chemical diffusion data. From this theory it follows that in the case under discussion the parabolic rate constant, k'_p , (expressed in $\text{cm}^2 \text{s}^{-1}$) is the product of nonstoichiometry and chemical diffusion coefficient [21, 22]:

$$k'_p = y \cdot \tilde{D} = [V''_{\text{Ni}}] \cdot \tilde{D} \quad (16)$$

Using this relationship and considering eqs. (14) and (15), the following k'_p dependence on oxygen pressure and temperature has been calculated:

$$k'_p = 0.028 \cdot p_{\text{O}_2}^{1/6} \cdot \exp\left(-\frac{232 \text{ kJ/mol}}{RT}\right) \quad (17)$$

It follows from this relationship that the calculated value of activation energy of nickel oxidation equals: $E_k = 232 \text{ kJ/mol}$. In order to compare these theoretical calculations with experimental results described by eq. (3), k'_p in eq. (17) should be recalculated into k_p by [25]:

$$k_p = 2 \left(\frac{M_{\text{O}}}{\bar{V} \cdot Z_{\text{O}}} \right)^2 k'_p \quad (18)$$

(where \bar{V} denotes the equivalent volume of NiO , M_{O} the atomic weight of oxygen, and Z_{O} the valency of anions) and the following relationship was obtained:

$$k_p = 0.12 \cdot p_{\text{O}_2}^{1/6} \cdot \exp\left(-\frac{232 \text{ kJ/mol}}{RT}\right) \quad (19)$$

From the comparison of eqs. (3) and (19) it follows clearly that the calculated value of parabolic rate constant of nickel oxidation, as dependent on temperature and oxygen pressure, is in excellent agreement with experimentally determined data. This agreement is even better visible in Fig. 9.

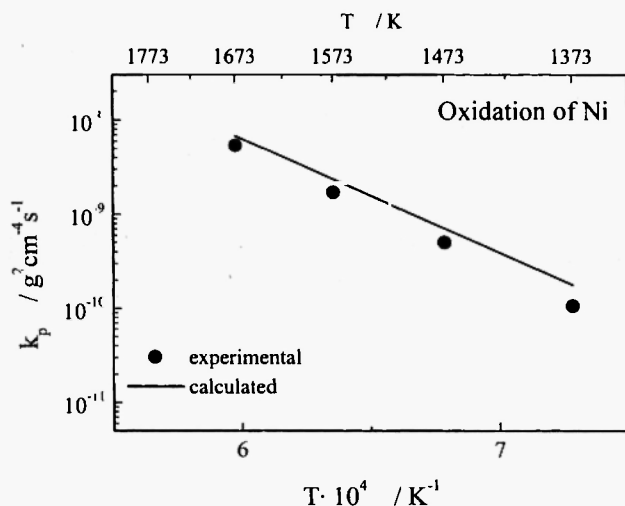


Fig. 9: The comparison of calculated parabolic rate constants of nickel oxidation with those, determined experimentally.

Considering eq. (18) the relationship, described by eq. (16), may be presented in the following modified form:

$$k_p = 2 \cdot \left(\frac{M_O}{\bar{V} \cdot Z_O} \right)^2 \cdot [V_{Ni}^*] \cdot \tilde{D} \quad (20)$$

This equation can be further modified utilizing eqs. (7) and (15):

$$k_p = 2 \left(\frac{M_O}{\bar{V} \cdot Z_O} \right)^2 \cdot \text{const} \cdot \dot{r}_{O_2}^{1/6} \cdot \exp \left(- \frac{\frac{1}{3} \Delta H_f + \Delta H_m}{RT} \right) \quad (21)$$

From this relationship it follows that the activation energy of nickel oxidation, E_k , is the sum of one third of the enthalpy of defect formation and the activation enthalpy of their migration in the growing Ni_{1-y}O scale. Thus, considering the results described by eqs. (14) and (15), activation energy of nickel oxidation may be calculated:

$$E_k = \frac{1}{3} \Delta H_f + \Delta H_m = 232 \text{ kJ/mol} \quad (22)$$

As can be seen, the calculated value of E_k is in

excellent agreement with that obtained experimentally (eq. (3)), once more confirming that double ionized cation vacancies dominate in nickel oxide and that the growth rate of Ni_{1-y}O scale on nickel is governed by the volume diffusion of cations.

From Wagner's theory it follows further that in the discussed case the parabolic rate constant expressed in $\text{cm}^2 \text{s}^{-1}$ k'_p is related to the self-diffusion coefficient of cations, D_{Ni} , in Ni_{1-y}O by the following simple relationship:

$$k'_p = (1 + |p|) \cdot D_{Ni} \quad (23)$$

where p is a degree of defect ionization (in the case under discussion $p = -2$). Thus, D_{Ni} can be calculated from k'_p as a function of temperature and oxygen pressure under the assumption that the rate determining step of nickel oxidation is the outward diffusion of cations through double ionized vacancies in the growing Ni_{1-y}O scale. Using this relationship and considering empirical eq. (17), self-diffusion coefficient of nickel in nickel oxide has been calculated as a function of temperature and oxygen pressure:

$$D_{Ni} = 9.3 \cdot 10^{-3} \cdot p_{O_2}^{1/6} \cdot \exp \left(- \frac{232 \text{ kJ/mol}}{RT} \right) \quad (24)$$

Fig. 10 illustrates the results of these calculations (solid line) in Arrhenius plot for oxygen pressure equal to 10^5 Pa on the background of experimentally determined D_{Ni} values obtained by several authors [13, 24, 26] at the same oxygen pressure. As can be seen, experimental results obtained using tracer method are in good agreement with calculated values in the present paper. This agreement strongly suggests that important information on transport properties of metal oxides can be obtained from simple oxidation rate measurements in contrast with rather difficult and time-consuming tracer experiments.

It has been found that the oxidation process of Ni-Cr and Ni-Na alloys, like that of pure nickel, follows strictly parabolic kinetics, being thus diffusion controlled. Figs. 11 and 12 show temperature and pressure dependence of the parabolic rate constant of Ni-1%Cr alloy oxidation on the background of

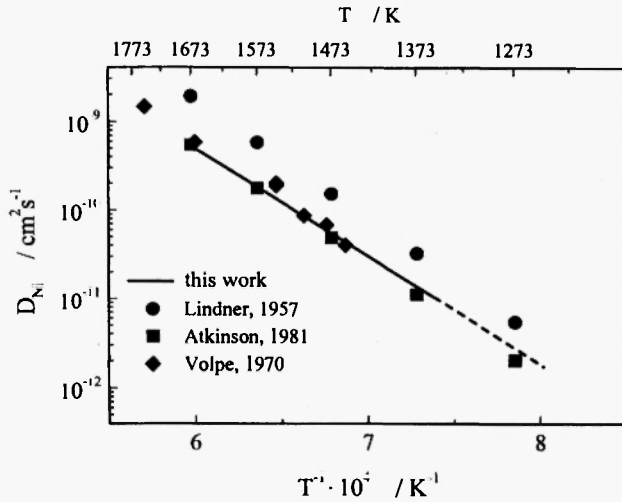
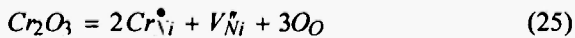


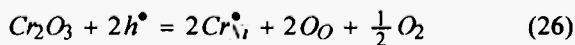
Fig. 10: The temperature dependence of calculated self-diffusion coefficient of nickel in Ni_{1-y}O on the background of experimental results obtained by several authors.

analogous results obtained for pure nickel. As can be seen, the oxidation rate of alloy is considerably higher than that of pure nickel and the activation energy of this process is lower (Fig. 11). In addition, the rate of alloy oxidation does not depend on oxygen pressure at all (Fig. 12).

These differences can be satisfactorily explained in terms of doping effect [27, 28], basing on defect model of Ni_{1-y}O described in the previous chapter. If, namely, one assumes that in the growing oxide scale on Ni-Cr alloy, double ionized cation vacancies and electron holes predominate and trivalent chromium ions are substitutionally incorporated into the cation sublattice of Ni_{1-y}O , this process can be described by the following quasi-chemical reversible reactions:



and



It follows from these defect equilibria, that the concentration of cation vacancies in chromium doped Ni_{1-y}O is higher than that in pure nickel oxide and the concentration of electron holes is lower. Consequently,

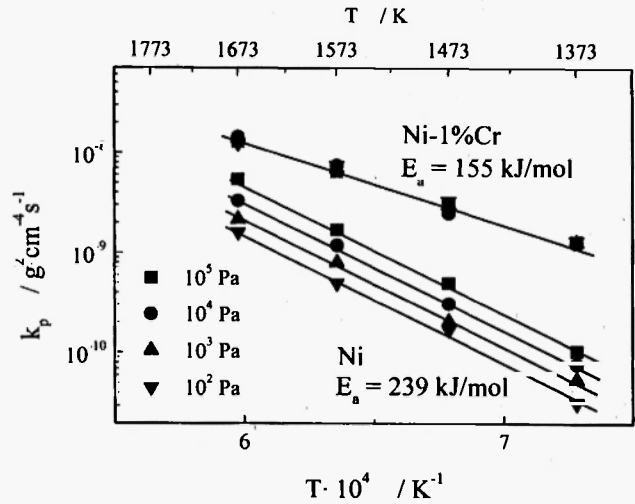


Fig. 11: The temperature dependence of the oxidation rate of the Ni-1%Cr alloy for several oxygen pressures.

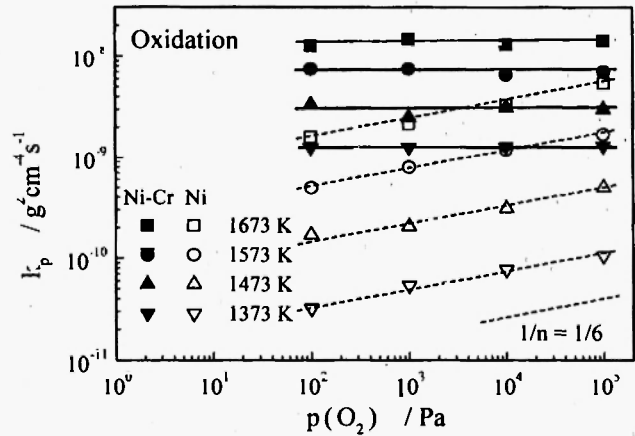


Fig. 12: The pressure dependence of the oxidation rate of the Ni-1%Cr alloy for several temperatures.

the growth rate of the scale on Ni-Cr alloy, composed of Cr_2O_3 - Ni_{1-y}O solid solution, should be higher than that of Ni_{1-y}O scale on pure nickel metal.

The electroneutrality condition for such Cr_2O_3 - Ni_{1-y}O solid solution is given by:

$$[\text{Cr}_{\text{Ni}}^{\bullet}] + [h^{\bullet}] = 2[V_{\text{Ni}}^{\bullet}] \quad (27)$$

Two limiting cases should be considered. If the concentration of dopant is too low to affect the intrinsic

ionic and electron disorder in Ni_{1-y}O ($[Cr_{Ni}^{\bullet}] \ll [h^{\bullet}]$), the above electroneutrality condition reduces to the following simplified form:

$$[h^{\bullet}] = 2[V_{Ni}^{\bullet}] \quad (28)$$

and the oxidation rate of alloy, as dependent on oxygen pressure and temperature, should be the same as that of pure nickel. On the other hand, when the dopant concentration is much higher than that of electronic defect ($[Cr_{Ni}^{\bullet}] \gg [h^{\bullet}]$), the electroneutrality condition (eq. (27)) assumes the following simplified form:

$$[Cr_{Ni}^{\bullet}] = 2[V_{Ni}^{\bullet}] \quad (29)$$

indicating that, in this case, the extrinsic region of defect situation has been reached, in which the concentration of cation vacancies is fixed by the dopant on the constant level. Both these defect situations, described by two limiting electroneutrality conditions (eqs. (28) and (29)) are shown schematically in Fig. 13, illustrating the influence of chromium on the defect structure in Ni_{1-y}O , as a function of equilibrium oxygen pressure, at constant temperature. It follows from this schematic diagram that with increasing temperature and oxygen pressure higher and higher dopant concentration is needed to pass from intrinsic (eq.(28)) to extrinsic (eq.(29)) region, because the concentration of native

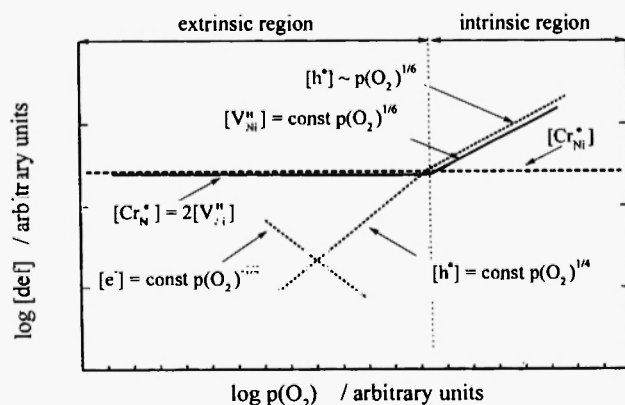


Fig. 13: Defect situation in chromium doped Ni_{1-y}O (schematic).

defects in Ni_{1-y}O increases with both these two parameters.

The results presented in Figs. 11 and 12 show clearly that in our case the amount of chromium, incorporated into the oxide scale, was high enough to fix the concentration of cation vacancies on the constant level, i.e. that the simplified electroneutrality condition described by eq. (29) was fulfilled. Consequently, the oxidation rate of Ni-Cr alloy containing 1 at % of Cr was higher than that of pure nickel (Fig. 11) and was pressure independent (Fig. 12).

In addition, from Fig.11 it follows also that the activation energy of alloy oxidation was lower than that of pure nickel. This important fact is also in agreement with theoretical predictions. From eq. (22) it follows, namely, that in the activation energy of pure nickel oxidation, both the enthalpy of defect formation and that of their migration in the growing scale participate, because not only defect mobility but also their concentration increases with increasing temperature. In the case of alloy oxidation, on the other hand, the concentration of cation vacancies is fixed by the dopant on the constant level and consequently $\Delta H_f = 0$. Thus, the activation energy of alloy oxidation must be lower than that of pure nickel oxidation and simply equal to the enthalpy of defect migration in the scale, ΔH_m . From eq. (15) it follows that $\Delta H_m = 152$ kJ/mol, which is in excellent agreement with E_a of Ni-Cr alloy oxidation (Fig. 11). It may then be concluded that the influence of chromium on the kinetics and mechanism of nickel oxidation can satisfactorily be explained in terms of doping effect. The fact that 1 at % of Cr was high enough to fix the concentration of cation vacancies in $\text{Ni}_{1-y}\text{O-Cr}_2\text{O}_3$ scale on the constant level is not surprising, because the concentration of native defects in pure Ni_{1-y}O is more than two orders of magnitude lower than that of dopant.

A different situation has been observed in the case of Ni-Na alloy oxidation. It has been found that the oxidation process also follows parabolic kinetics, being thus diffusion controlled, but the rate of reaction was lower and increased more rapidly with oxygen pressure than in the case of pure nickel oxidation (Fig. 14). In addition, the activation energy of reaction was higher (Fig. 15). These results may again be explained in terms of doping effect. Assuming, namely, that the univalent

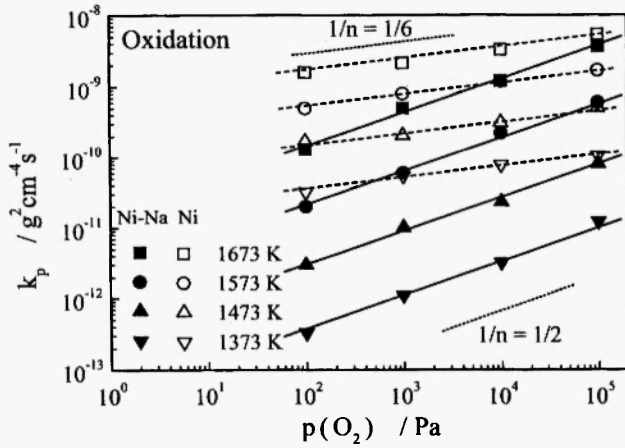


Fig. 14: The pressure dependence of the oxidation rate of the Ni-Na alloy for several temperatures.

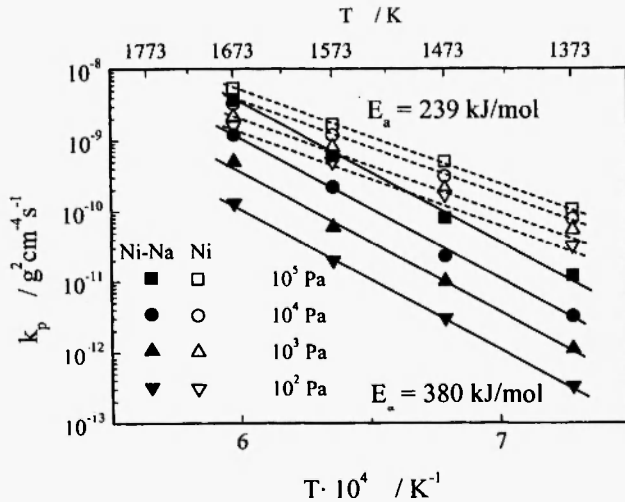
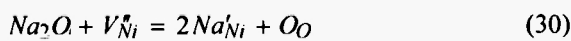
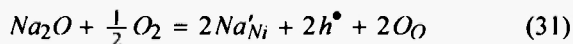


Fig. 15: The temperature dependence of the oxidation rate of the Ni-Na alloy for several oxygen pressures.

sodium ions are incorporated substitutionally into the cation sublattice of Ni_{1-y}O , this process can be described by the following reversible defect reactions:



and



From these defect equilibria it follows that, in contrast to chromium doping, the concentration of cation vacancies in sodium doped Ni_{1-y}O should be lower and the concentration of electron holes higher, than those in pure nickel oxide. The electroneutrality condition for this case assumes the form:

$$[\text{Na}'_{\text{Ni}}] + 2[V_{\text{Ni}}^*] = [h^\bullet] \quad (32)$$

Two limiting cases should again be considered. If $[\text{Na}'_{\text{Ni}}] \ll [V_{\text{Ni}}^*]$, the electroneutrality condition reduces to the following simplified form:

$$[h^\bullet] = 2[V_{\text{Ni}}^*] \quad (33)$$

which implies that the dopant concentration is too low to affect the intrinsic ionic and electronic disorder in Ni_{1-y}O . On the other hand, when $[\text{Na}'_{\text{Ni}}] \gg [V_{\text{Ni}}^*]$, the electroneutrality condition assumes the form:

$$[\text{Na}'_{\text{Ni}}] = [h^\bullet] \quad (34)$$

This implies that the concentration of electronic defects in such $\text{Na}_2\text{O-Ni}_{1-y}\text{O}$ solid solution is fixed by the presence of dopant on the constant level and the concentration of cation vacancies is much lower than that in pure Ni_{1-y}O , increasing more rapidly with oxygen pressure. This last conclusion results directly from the application of mass action law to the defect reaction described by eq. (4):

$$K_V = [V_{\text{Ni}}^*] \cdot [h^\bullet]^2 \cdot p_{\text{O}_2}^{1/2} \quad (35)$$

Replacing in this relationship the electron hole concentration by that of dopant (eq. (34)) and eliminating the equilibrium constant K_V yields:

$$[V_{\text{Ni}}^*] = \frac{1}{[\text{Na}'_{\text{Ni}}]^2} \cdot p_{\text{O}_2}^{1/2} \cdot \exp\left(\frac{\Delta S_f}{R}\right) \cdot \exp\left(-\frac{\Delta H_f}{RT}\right) \quad (36)$$

As the parabolic rate constant of oxidation is directly proportional to the concentration of cation vacancies in the growing scale, the oxidation rate of Ni-Na alloy should be lower than that of pure nickel and increase

more rapidly with oxygen pressure and temperature, which is in agreement with experimental results, shown in Figs. 14 and 15.

From eq. (36) it follows that the influence of dopant at constant temperature depends not only on its concentration but also on oxygen pressure. Thus, at any constant sodium concentration both limiting cases (eq. (33) and (34)) may theoretically be realized, as in the case of chromium (Fig. 13), by appropriate changes of equilibrium oxygen pressure, as shown schematically in Fig. 16. In the intrinsic region (higher oxygen pressures) the concentration of dopant is too low to affect the defect structure of Ni_{1-y}O and the oxidation rate of alloy would be the same as that of pure nickel (eq. (33)). With decreasing oxygen activity, the concentration of point defects in the oxide decreases and at sufficiently low oxygen pressure the extrinsic region may be reached, in which the dopant determines the electron hole concentration (eq. (34)). The lower the dopant concentration, the lower the oxygen pressure needed to pass from the intrinsic to the extrinsic region. From the results shown in Figs. 14 and 15 it follows clearly that the concentration of sodium was high enough to reach the extrinsic region, as the oxidation rate of alloy was lower than that of pure nickel and increased more rapidly with oxygen pressure with the slope 2. This conclusion could have been expected because the concentration of point defects in Ni_{1-y}O was at least one order of magnitude lower than that of dopant.

In addition, it has been found that the activation energy of alloy oxidation was higher than that of pure

nickel, as illustrated in Fig. 15. This difference is again in agreement with theoretical predictions. As already mentioned, activation energy of pure nickel oxidation is the sum of enthalpy of defect formation, ΔH_f , and activation enthalpy of their migration, ΔH_m , in the oxide scale. In this case, the concentration of both, ionic and electronic defects increase with increasing temperature and only one third of ΔH_f (eq. (21)) participates in the activation energy of cation self-diffusion and thereby in the activation energy of Ni oxidation. In sodium doped Ni_{1-y}O , on the other hand, if the dopant content is sufficiently high, the electron hole concentration is fixed on the constant level (eq. (34)), and consequently the temperature dependence of the concentration of ionic defects is described by eq. (36). It follows from this relationship that the concentration of cation vacancies in $\text{Na}_2\text{O-Ni}_{1-y}\text{O}$ solid solution must increase more rapidly, not only with increasing oxygen pressure but also with temperature, because the whole value of ΔH_f participates in the activation energy of alloy oxidation:

$$\begin{aligned} E'_p &= E'_D = \Delta H_f + \Delta H_m > E_p \\ &= E_D = \frac{1}{3} \Delta H_f + \Delta H_m \end{aligned} \quad (37)$$

where E'_p and E'_D denote the activation energy of Ni-Na alloy oxidation and that of self diffusion of cations in $\text{Na}_2\text{O-Ni}_{1-y}\text{O}$ solid solution, respectively. If one assumes that enthalpies of defect formation and their migration in pure and sodium doped Ni_{1-y}O are the same, E'_p may simply be estimated from the following relationship:

$$E'_p = \Delta H_f + \Delta H_m \quad (38)$$

From the comparison of eqs. (7) and (14) it follows that $\Delta H_f = 240$ kJ/mol. On the other hand, activation enthalpy of defect migration has been found to be: $\Delta H_m = 152$ kJ/mol [15]. Introducing these two values into eq. (38), one obtains the following activation energy of alloy oxidation: $E'_p = 392$ kJ/mol, which is in satisfactory agreement with experimental results (Fig. 15).

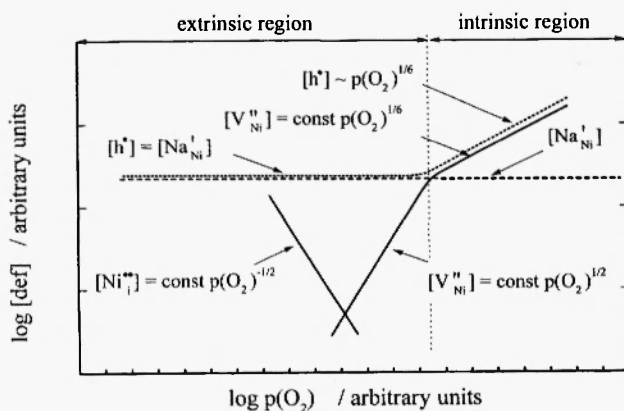


Fig. 16: The influence of univalent dopant on the defect situation in Ni_{1-y}O (schematic).

4. CONCLUSIONS

The results described in the present paper allow the following conclusions to be formulated.

The growth process of coarse grained oxide scale on nickel is governed by the outward volume diffusion of cations and the participation of grain boundary diffusion in this reaction may be neglected. Farther, from the pressure dependence of the oxidation rate of nickel and that of nonstoichiometry of nickel oxide, it follows that the predominant defects in Ni_{1-y}O are doubly ionized cation vacancies and electron holes. Thus, some remarks in the literature concerning complex defect structure in this oxide have not been confirmed in the present work. It may be then concluded that these remarks results from the influence of impurities in the studied materials, as suggested by Rapp [16] and Kofstad [3], as well as from fine grained character of Ni_{1-y}O samples used in those studies.

Very good agreement between calculated and experimentally determined parabolic rate constant of nickel oxidation and self-diffusion coefficient of Ni in nickel oxide clearly indicates that from rather simple oxidation rate measurements important information may be formulated, concerning both the mechanism of metal oxidation as well as the defect structure and transport properties of oxides forming the scales. However, reasonable conclusions may only be formulated if very high purity metal is utilized in oxidation studies and the experiments are carried out in such a way that in the whole temperature range the coarse-grained scale is formed. Also, coarse-grained oxide samples, obtained from metal oxidation at very high temperatures, must be used in nonstoichiometry and chemical diffusion studies.

It has been shown that the influence of aliovalent impurities on the oxidation rate of nickel and on the defect structure of metal deficit nickel oxide (Ni_{1-y}O) may satisfactorily be explained in terms of doping effect. If, namely, the amount of trivalent dopant is high enough to fix the concentration of cation vacancies on a constant level, the oxidation rate of diluted Ni-Cr alloy does not depend on oxygen pressure and is higher than that of pure nickel. In addition, the activation energy of this process is lower and equal to the activation enthalpy of defect migration in the growing scale. On the other

hand, the sufficiently high univalent dopant concentration stabilizes the concentration of electron holes and reduces the concentration of ionic defects. As a consequence, the oxidation rate of diluted Ni-Na alloy is lower than that of pure nickel and increases more rapidly with oxygen pressure as well as the activation energy is higher.

Very good agreement between calculated and experimentally found activation energies of the oxidation of Ni-Cr and Ni-Na alloys, as well as the pressure dependence of the oxidation rates, confirms the conclusion that the predominant defects in nonstoichiometric nickel oxide (Ni_{1-y}O) are double ionized cation vacancies and electron holes. In addition, the obtained results strongly suggest that the aliovalent dopants used in this study dissolve substitutionally and not interstitially in the cation sublattice of nickel oxide. Finally, the above agreement confirms once again the possibility of applying Wagner's theory of metal oxidation in explaining in a rather simple way the influence of aliovalent impurities on defect and transport properties of nonstoichiometric metal oxides.

ACKNOWLEDGMENTS

This work was supported by the State Committee for Scientific Research in Poland no. 7T08A05220.

REFERENCES

1. R. Haugsrud, *Corr. Sci.*, **45**, 211 (2003).
2. D. Caplan, M. J. Graham and M. Cohen, *J. Electrochem. Soc.*, **119**, 1265 (1972).
3. P. Kofstad, *High Temperature Corrosion*, Elsevier Applied Science, London and New York, 1988, p. 212.
4. N. L. Peterson, *Solid State Ionics*, **12**, 201 (1984).
5. R. Hausgrud, T. Norby, *Solid State Ionics*, **111**, 323 (1998).
6. E. G. Moya, G. Deyme, F. Moya, *Scr. Metall. Mater.*, **24**, 2447 (1990).
7. C. Dubois, C. Monty, J. Philibert, *Phil. Mag. A*, **46**, 419 (1982).
8. P. Kofstad, *Nonstoichiometry. Diffusion and*

- Electrical Conductivity in Binary Metal Oxides*, J. Wiley, New York, 1972.
9. S. P. Mitoff, *J. Chem. Phys.*, **35**, 882 (1961).
 10. Y. D. Tretyakov and R. A. Rapp, *Trans. AIME*, **245**, 1235 (1969).
 11. W. C. Tripp and N. M. Tallan, *J. Am. Ceram. Soc.*, **53**, 531 (1970).
 12. R. Farhi and G. Petot-Ervas, *J. Phys. Chem. Solids*, **39**, 1169, (1978).
 13. Atkinson and R. I. Taylor, *Philos Mag. A*, **39**, 581 (1979); **43**, 979 (1981).
 14. M. L. Volpe, N. L. Peterson and J. Reddy, *Phys. Rev. B*, **3**, 1417 (1971).
 15. P. Kofstad, *High Temperature Corrosion*, Elsevier Applied Science, London and New York, 1988, p. 100.
 16. R. A. Perkins and R. A. Rapp, *Metallurgical Trans.*, **4**, 193 (1973).
 17. J. B. Wagner, Chemical Diffusion in Nonstoichiometric Compounds, in: *Mass Transport in Nonmetallic Solids*, *Proc. Brit. Ceram. Soc.*, **19**, 29 (1971).
 18. S. Mrowec and K. Hashimoto, *J. Mater. Sci.*, **30**, 4801 (1995).
 19. S. Mrowec and Z. Grzesik, *J. Phys. Chem. Solids*, **64**, 1387 (2003).
 20. S. Mrowec, Z. Grzesik and J. Dabek, *High Temp. Materials and Processes*, **21**, 87 (2002).
 21. P. Kofstad, *High Temperature Corrosion*, Elsevier Applied Science, London and New York, 1988, p. 172.
 22. S. Mrowec, *An Introduction to the Theory of Metal Oxidation*, National Bureau of Standards and National Science Foundation, Washington D. C., 1982, p. 172.
 23. F. Kröger, *The Chemistry of Imperfect Crystals*, North-Holland, Amsterdam, 1964.
 24. M. Volpe and J. Reddy, *J. Chem. Phys.*, **53**, 1117 (1970).
 25. S. Mrowec, *Defects and Diffusion in Solids*, Elsevier, Amsterdam - Oxford - New York, 1980.
 26. R. Linder and A. Åkerström, *Disc. Faraday Soc.*, **23**, 133 (1957).
 27. P. Kofstad, *High Temperature Corrosion*, Elsevier Applied Science, London and New York, 1988, p. 342.
 28. S. Mrowec, *An Introduction to the Theory of Metal Oxidation*, National Bureau of Standards and National Science Foundation, Washington D. C., 1982, p. 232.
 29. C. Wagner, *Atom Movements*, ASM Cleveland Ohio, 1951.